JPSE (Journal of Physical Science and Engineering), Vol. 7, No. 2, 2022, Page 68–74.
DOI: 10.17977/um024v7i22022p068

JPSE
(Journal of Physical Science and Engineering)

http://journal2.um.ac.id/index.php/jpse
EISSN: 2541-2485

Hydrogenated Amorphous Silicon Density of State Analyzed by Dielectric Function Model Derived from Ellipsometric Spectroscopy

Received
05 July 2022

Revised
19 July 2022

Accepted for Publication
27 July 2022

Published
21 October 2022

S Prayogi[1,2*], Y Cahyono[2], and Darminto[2,3]

1. Department of Electrical Engineering, Faculty of Industrial Technology, Pertamina University, Jl. Teuku Nyak Arief, Jakarta, 12220, Indonesia.
2. Department of Physics, Faculty of Science and Data Analytics, Institut Teknologi Sepuluh Nopember, Jl. Teknik Kimia, Surabaya, 60111, Indonesia.
3. Center of Excellence in Automotive Control and System, Institut Teknologi Sepuluh Nopember, Jl. Teknik Kimia, Surabaya, 60111, Indonesia.

***E-mail:** soni.prayogi@universitaspertamina.ac.id

This work is licensed under a Creative Commons Attribution-ShareAlike 4.0 International License

Abstract
In this study, we report the application of a functional dielectric model of scalable ellipsometric spectroscopy to investigate the optical response of materials in the optical spectrum modeling of hydrogenated amorphous silicon. ES is used to obtain the dielectric constant of the data fitting experimental. Then ψ and Δ are obtained from the analysis of the experimental comparison of the valence band and the conduction band state density with the band structure theory for a-Si: H. The analysis results are that for a-Si: H, the density of state model for all electronic transitions is obtained, whose results are consistent with experimental data from ES measurements over the entire photon energy range of 0.5–6.5 eV. Our results demonstrate the high-energy excitons and plasmons for the performance of photovoltaic devices in a-Si: H. Overall, we believe our methodology can study in detail about electron and hole interactions in semiconductors.
Keywords: a-Si: H, density of state, ellipsometric spectroscopy, chemical gap.

1. Introduction

Amorphous silicon (a-Si) differs from crystalline silicon (c-Si) in terms of the periodic range of its constituent atoms [1]. The arrangement of the atoms in amorphous matter is not random, but there is order in the short term. In a-Si, most of the atoms of silicon are four-fold and coordinated with a tetrahedral bond system similar to crystalline silicon [2]. The randomness of the method is formed due to variations in bond angles and long bonds, leading to long-term irregularities [3]. Compared to a-Si materials, hydrogenated amorphous silicon (a-Si: H) material has a lower defect density, making it easier to doping, and has higher photoconductivity [4]. That is advantageous if used as a solar cell with a p-i-n structure [5]. A thin layer of a-Si: H is suitable for application as a constituent component of solar cells [6]. This material has a broad optical energy band gap value (1.7–2 eV), a low growing temperature (~200 °C), and can be grown above [7]. Besides cheap glass substrates and abundant supplies, a-Si: H also has a high absorption ability in the visible light spectrum.

The physical phenomenon of solid-state is how the interaction between the optical properties of a material with the basic properties of the material [8]. Indeed, various models have been proposed over the years that attempt this [9]. This model is divided into two categories, the first is an empirical model, namely the relevance of experimental data and the second is physics principles [10]. The weakness of this empirical model lies in the fact that there is convergence to reach suitability, which is inferior to the experimental results [11]. Based on several adjustment parameters defined simultaneously, it is obtained that the physical model is generally complex and requires many parameters and calculations.

Our research is on how to get an accurate calculation model to see the optical response in a-Si [12]. In the a-Si material structure, the covalent bonds continuously make the four atoms coordinated in the binding configuration, we performed amorphous $\varepsilon(E)$ data analysis to a dielectric function model that is based on crystalline silicon [13]. Our findings show a correct fit of the spectroscopic ellipsometry

measurement spectrum with the calculated critical point in the energy of the crystalline material value [14]. An analysis is presented for a-Si: H and the important implications of this finding are considered.

2. Method

Thin film a-Si: H was grown on ITO substrate using PECVD with various hydrogen doping [15], as shown in Figure 1. The total deposition time for each film was kept constant at 30 minutes. The deposition parameters for the dilution of hydrogen SiH_4/H_2 are 0, 16, and 36, RF power 10 W, substrate temperature 270 °C, and process pressure (PP) 2000 mTorr. For R-0, no hydrogen dilution was carried out during precipitation. While for R-16 and R-36, hydrogens were diluted for 30 minutes. The thin film conductivity was measured using a four-point probe method coupled with a conductive layer of silver paste on each a-Si: H thin film [16].

The ellipsometry spectroscopy (ES) parameters ψ and Δ with measuring angles at 50°, 60°, and 70° of incidence, at the length of the photon energy between 0.6 and 6.5 eV. The results of spectroscopic ellipsometry measurements are real and imaginary components that explain the condition of the optically measured material. Because it requires more in-depth information, further analysis is required with the help of the analysis software Woollam Complete Ease. The parameters correspond to the surface roughness of the R-0, R-16, and R-36 samples. The parameterization of each that can be analyzed through the software is the dielectric function of the measurement which aims to determine the thickness, band gap, and optical constant of the film [17]. This complex dielectric function can be used for optical properties of a-Si: H materials related to the angular frequency of incident photons.

3. Result and Discussion

Measurement of the surface morphology of a-Si: H was carried out using an AFM instrument which was used to see the surface texture and roughness of the deposited a-Si: H thin film. During the AFM measurement process, the tip will move along the surface of the test material causing the cantilever slope to vary. The slope of the cantilever will be detected by the photodetector. The laser beam given to the cantilever will be received by the detector which will be detected as the cantilever slope. Measurement or scanning is taken at the boundary of the layer and substrate (no coating). This slope change will provide depth information. Scanning in this border area will get information on the difference in height or depth which states the thickness of the thin layer formed [18]. Figure 2 shows the line profiles and surface topographies of the R-0, R-16, and R-36 samples with roughness values of 8.95, 6.20, and 3.50 nm, respectively. Here it is seen that the increase in deposition rate is caused by the increase in electron density in the plasma so that the radical density near the substrate also increases.

The parameters of the model's dielectric function specified a-Si are listed in Table 1. The data shows that there are characteristics between c-Si and a-Si. This gap is not the result of a critical point energy gap but is thought to arise from a sequence of short distances defined by covalent bonds. The clearly observed term between the optical spectrum of amorphous silicon, which is an electronic lattice and a vibrational lattice, can generally be interpreted in terms of symmetrical arguments based on measurements from low to high energy [19]. If the short-range arrangement in the amorphous state is similar to the arrangement in the corresponding of crystal, one would expect the density of state (DOS)

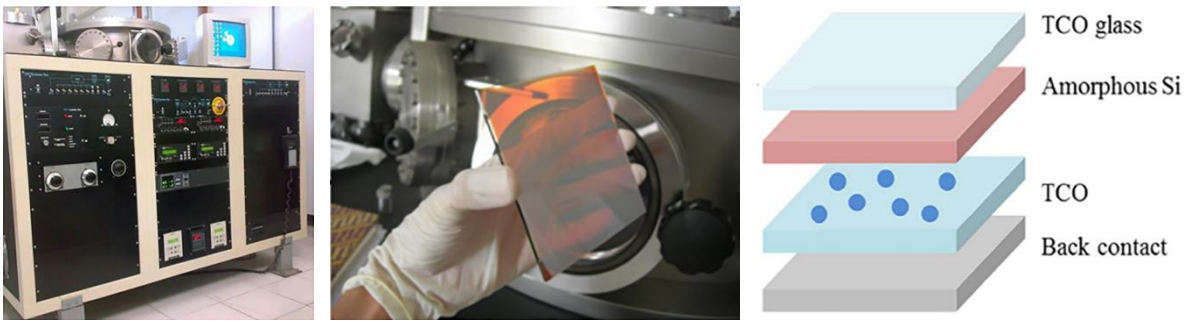

(a) (b) (c)

Figure 1. Schematic of amorphous silicon sample preparation. (a) Multiple chamber RF-PECVD system, (b) amorphous silicon sample (10 × 10) cm^2 is integrated with a conductive film, and (c) schematic diagram of a-Si: H.

electronics and phonons to show some similarity to the crystal [20] Basically, the density of the amorphous material is the parent function of the crystalline material as in Figure 3. From the results obtained, it is shown that the crystal structure can also be applied to amorphous materials without special precautions.

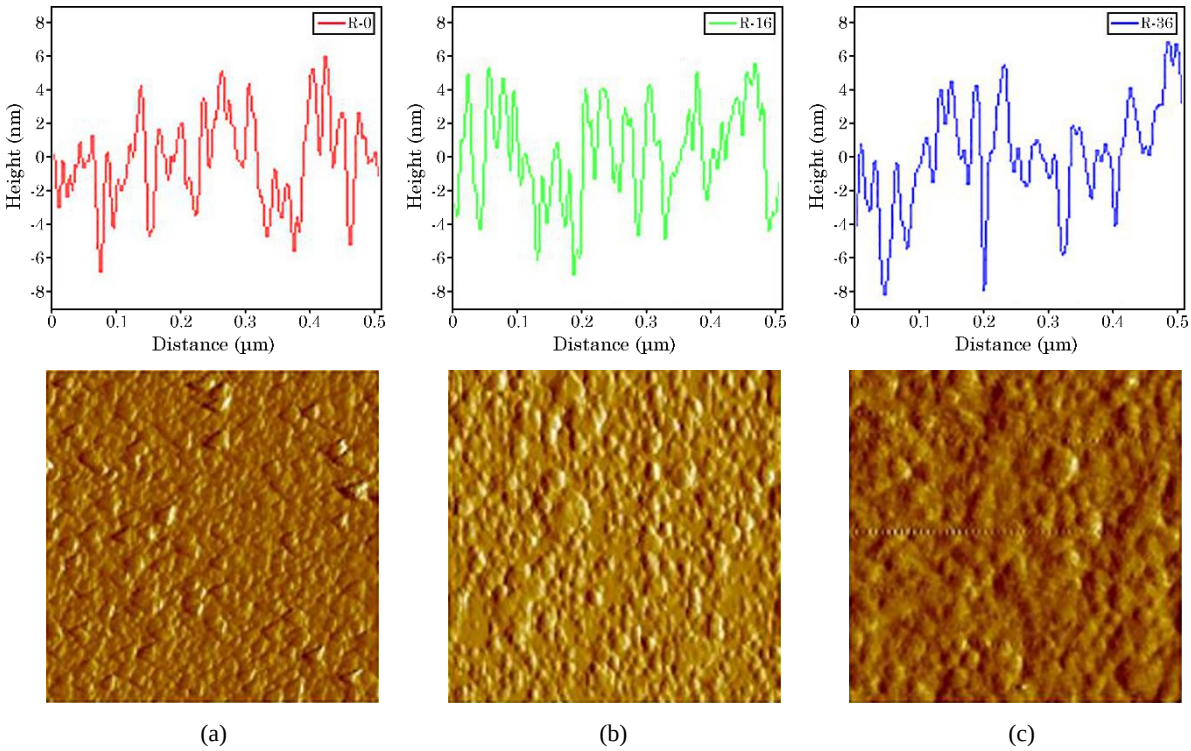

Figure 2. Line profiles and AFM topography images on the samples with (a) R-0, (b) R-16, and (c) R-36.

Table 1. Critical-point indicator in the calculation of $\varepsilon(E)$ for a-Si [21].

Parameters	a-Si
E_1 (eV)	2.90
B_1	5.36
B_{1x} (eV^2)	1.74
E_2 (eV)	4.14
E_o' (eV)	2.61
E_1' (eV)	5.0

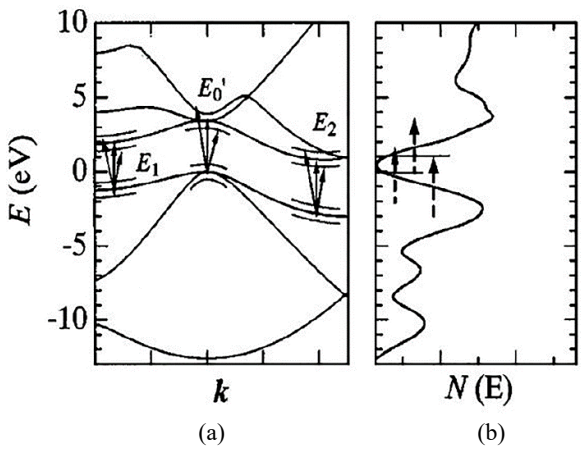

Figure 3. (a) Electronic structure of the band structure, and (b) the density of state a-Si [22].

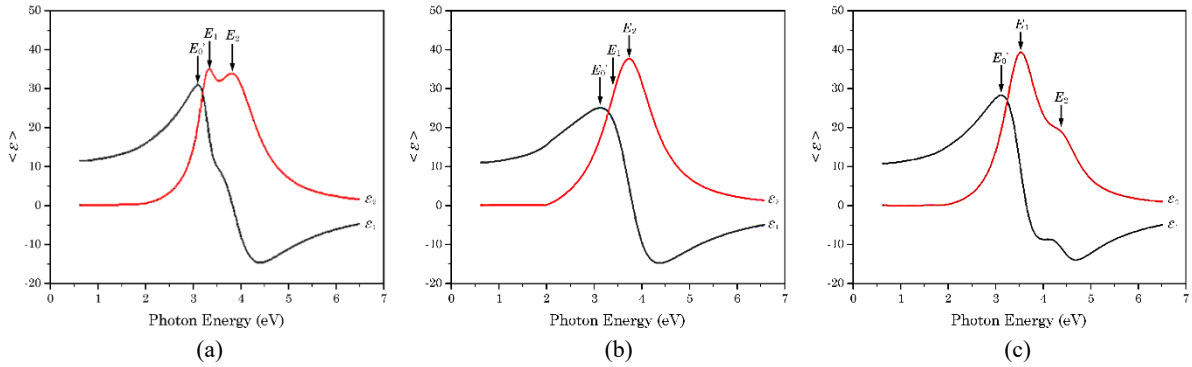

Figure 4. Imaginary part <ε_2> of the dielectric function for (a) R-0, (b) R-16, and (c) R-36.

For samples R-0, the peak of the ε_2 shift graph or the excitons shift is E_1 = 3.34 eV and E_2 = 3.82 eV. In the c-Si to R-0, the second excitons pushed into spectral weight at low energy and visible presence ε_2 broadening on the magnitude of the shift of 0.48 eV. So, it is said that the c-Si condition to R-0 is called the quantum confinement effect, as in Figure 4a. Namely the coupling between excitons. It proves that quantum confinement occurs in both excitons. It is consistent with the ε_2 and band structure [23], where the transmission changes from high energy crossing zero to low energy with a significant energy shift of 1.84 eV. There must be a spectral weight transfer at ε_2 R-0, whereas the c-Si does not exist. It turns out that on the ε_2 c-Si graph at high energy, namely at 3.09 eV, there is a transfer of energy to the low energy of 3.34 eV, which causes a spectral weight transfer of 3.82 eV, which is often called electronic signature correlations.

To confirm this, we tried to fit our measured a-Si $\varepsilon(E)$ spectrum with a model dielectric function calculation. Figure 4 shows the results of this fit imaginary part <ε_2> of the dielectric function. The model dielectric function parameters that were determined accordingly are listed in Table 1. The key finding for achieving a good fit between the calculated and experimental a-Si $\varepsilon_2(E)$ spectra is using CP energies that are different from crystal energies. In fact, only an increase in the expansion parameter corresponds poorly to the experimental data, as shown in Figure 3b with a dashed line.

In the R-0 to R-16 graph, there is not only the quantum confinement effect but the dramatic effect of hydrogen. At the peak of the second excitons shift to high energy, while the peak of the first excitons shift is almost the same as the second excitons. As a result, two collabs excitons coincide. The same thing in the loss function R-16 is a coupling between excitons and plasmons. In Figure 4b and Figure 4c, when there is another addition of hydrogen, spectral weight transfer occurs again on the ε_2 R-36 graph with an energy of 4.43 eV. That causes the excitons to return to the original. Where the difference in the initial conditions of the excitons occurred at 3.38 eV at R-0 to 3.58 eV at R-36. This means that the function of hydrogen here seems to be returning to its bulk-like properties [24]. So, the hydrogen function here, although thin, can restore the primary function, or it can also be said to be the hydrogen function to regulate electronic correlations, along with that in plasmons, it also occurs.

In general, the results of XPS and BIS measurements for c-Si and a-Si have been carried out by previous researchers [22]. Here we show the density of crystalline and amorphous compare their spectra with the general theory [22]. Meanwhile, the XPS and BIS measurements that have been obtained are useful for investigate the valence band and conduction band at density of c-Si and a-Si states. In the results obtained, it turns out that the results are very consistent with those carried out using a spectroscopic [25]. These results are combined in Figure 5, The positions of several important electronic states at the density of states in c-Si and a-Si are also shown in Figure 5. It is clear here that the CP between the high energy band and the low energy band for a-Si is consistent with measurements using a spectroscopic ellipsometry, also shown in Figure 5. On the other hand, we find that the characteristic gap in this amorphous form arises from the short wavelength defined by the covalent bond.

Confirmation of the critical points E_1 and E_2, for the c-Si structure, is shown on the dotted line of the characteristics used for the calculation of the dielectric function model of the a-Si structure. In Figure 5, The first valence band in the a-Si structure consists of two peaks of the ellipsometer spectroscopic measurement graph, and the conduction band is also analyzed. We can also see in Figure 4b that the changes that occur are caused by the electronic properties of the c-Si and a-Si structures. The relatively

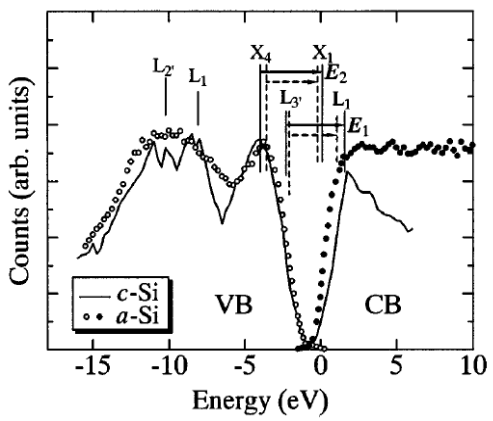

Figure 5. Results of XPS and BIS measurements for c-Si and a-Si [21].

stable energy shift from the density peaks in the a-Si structure results from the bond angle interactions. [26]. The resulting energy value causes a significant change in the a-Si structure (Table 1) probably mainly due to density variations in this structure. Our analysis shows that the order in the low energy band conditions is determined by covalent bonds, while the optical spectrum in the crystalline structure and amorphous structure uses variations at high energy and low energy [27]. It is not surprising given the fact that short-range orders in amorphous materials produce Raman peaks and x-ray diffraction (XRD) [28]. Here it is found, if the energy peaks are not correlated with the order of short distances, then there is no peak that occurs in the amorphous material.

4. Conclusion

Dielectric function and DOS models have been analyzed to model the optical response in a-Si: H. It is obtained that the a-Si: H results show a specific band structure confirmed by the high-resolution XPS spectrum. The resulting analysis is consistent and has been applied to other amorphous materials. Therefore, we can suppose that short-range sequences are essential to discuss the optical properties of crystalline and amorphous substances. The scattering of electrons from coupling high-energy excitons and plasmons increases bulk carrier density and, subsequently, a reversible shift in Fermi energy. Our results demonstrate the high-energy excitons and plasmons for the performance of photovoltaic devices in a-Si: H. Overall, we believe our methodology can study in detail electron and hole interactions in semiconductors

Acknowledgment

The authors would like to thank Pertamina University for its support and facilities.

References

[1] R. E. I. Schropp, “Industrialization of hot wire chemical vapor deposition for thin film applications,” *Thin Solid Films*, vol. 595, pp. 272–283, Nov. 2015, doi: 10.1016/j.tsf.2015.07.054.

[2] A. Biswas *et al.*, “Spectroscopic ellipsometry studies of reactively sputtered nitrogen-rich GaAsN films,” *J. Non-Cryst. Solids*, vol. 357, no. 18, pp. 3293–3300, Sep. 2011, doi: 10.1016/j.jnoncrysol.2011.06.007.

[3] A. Listanti, A. Taufiq, A. Hidayat, and S. Sunaryono, “Investigasi struktur dan energi band gap partikel nano TiO2 hasil sintesis menggunakan metode sol-gel,” *JPSE (J. Phys. Sci. Eng.)*, vol. 3, no. 1, pp. 8–15, Apr. 2018, doi: 10.17977/um024v3i12018p008.

[4] S. Prayogi, Y. Cahyono, and D. Darminto, “Electronic structure analysis of a-Si: H p-i_1-i_2-n solar cells using ellipsometry spectroscopy,” *Opt. Quantum Electron.*, vol. 54, no. 11, p. 732, Sep. 2022, doi: 10.1007/s11082-022-04044-5.

[5] S. Prayogi, Y. Cahyono, I. Iqballudin, M. Stchakovsky, and D. Darminto, “The effect of adding an active layer to the structure of a-Si: H solar cells on the efficiency using RF-PECVD,” *J.*

Mater. Sci. Mater. Electron, vol. 32, no. 6, pp. 7609–7618, Mar. 2021, doi: 10.1007/s10854-021-05477-6.

[6] N. Nair *et al.*, "Influence of the properties of p-a-Si:H layer and the work function of front contact on silicon heterojunction solar cell performance," *Mater. Today Proc.*, vol. 49, pp. 1617–1624, Jan. 2022, doi: 10.1016/j.matpr.2021.07.421.

[7] X. Wang *et al.*, "Impacts of the a-Si:H interlayer nanostructure on the adhesion of the thick DLC coatings prepared by PECVD," *Appl. Surf. Sci.*, vol. 565, p. 150539, Nov. 2021, doi: 10.1016/j.apsusc.2021.150539.

[8] K. W. Mas'udah, F. Astuti, and D. Darminto, "Study on physical properties of reduced graphene oxide from heating coconut shell," *JPSE J. Phys. Sci. Eng.*, vol. 1, no. 1, pp. 1–6, Dec. 2016, doi: 10.17977/um024v1i12016p001.

[9] D. Hamdani, S. Prayogi, Y. Cahyono, G. Yudoyono, and D. Darminto, "The effects of dopant concentration on the performances of the a-SiO_x:H(p)/a-Si:H(i_1)/a-Si:H(i_2)/μc-Si:H(n) heterojunction solar cell," *Int. J. Renew. Energy Dev.*, vol. 11, no. 1, pp. 173–181, Feb. 2022, doi: 10.14710/ijred.2022.40193.

[10] S. Solehudin, *et al*, "Analysis of nanoporous semiconductor film thickness effect on short circuit current density of β-carotene dye based DSSC: Theoretical and experimental approach," *JPSE (J. Phys. Sci. Eng.)*, vol. 4, no. 1, pp. 1–7, Jun. 2020, doi: 10.17977/um024v4i12019p001.

[11] D. Hamdani, S. Prayogi, Y. Cahyono, G. Yudoyono, and D. Darminto, "The influences of the front work function and intrinsic bilayer (i1, i2) on p-i-n based amorphous silicon solar cell's performances: A numerical study," *Cogent Eng.*, vol. 9, no. 1, p. 2110726, Aug. 2022, doi: 10.1080/23311916.2022.2110726.

[12] Z. Dorostghol and A. Kosarian, "Improving structural, optical, and electrical properties of μc-Si:H using non-uniform hydrogen dilution treatment on RF-PECVD prepared layers," *Mater. Sci. Semicond. Process*, vol. 129, p. 105790, Jul. 2021, doi: 10.1016/j.mssp.2021.105790.

[13] K. Bendjebbar, W. L. Rahal, D. Rached, and S. Bahlouli, "Numerical analysis of metal-semiconductor junctions ITO/p-a-Si:H and n-c-Si/Al on silicon heterojunction solar cells," *Optik*, vol. 212, p. 164741, Jun. 2020, doi: 10.1016/j.ijleo.2020.164741.

[14] Y. Luo, M. Lin, N. Zhou, H. Huang, C.-T. Tsai, and L. Zhou, "Molecular dynamics simulation study of the microstructure of a-Si:H thin film grown by oblique-angle deposition," *Phys. B Condens. Matter*, vol. 545, pp. 80–85, Sep. 2018, doi: 10.1016/j.physb.2018.05.042.

[15] S. Prayogi, M. A. Baqiya, Y. Cahyono, and Darminto, "Optical transmission of p-type a-Si:H thin film deposited by PECVD on ITO-coated glass," *Mater. Sci. Forum*, vol. 966, pp. 72–76, Aug. 2019, doi: 10.4028/www.scientific.net/MSF.966.72.

[16] Y. Cahyono, E. Yahya, M. Zainuri, S. Pratapa, and Darminto, "Quantum confinement in an intrinsic a-Si:H thin film deposited on soda lime glass substrate using PECVD," *Trans. Electr. Electron. Mater.* vol. 19, no. 1, pp. 69–73, Feb. 2018, doi: 10.1007/s42341-018-0002-3.

[17] S. Prayogi, Ayunis, Kresna, Y. Cahyono, Akidah, and Darminto, "Analysis of thin layer optical properties of A-Si:H P-Type doping CH_4 and P-Type without CH_4 is deposited PECVD systems," *J. Phys. Conf. Ser.*, vol. 853, p. 012032, May 2017, doi: 10.1088/1742-6596/853/1/012032.

[18] D. Franta, I. Ohlídal, P. Klapetek, and P. R. i Cabarrocas, "Complete characterization of rough polymorphous silicon films by atomic force microscopy and the combined method of spectroscopic ellipsometry and spectroscopic reflectometry," *Thin Solid Films*, vol. 455–456, pp. 399–403, May 2004, doi: 10.1016/j.tsf.2003.11.237.

[19] S. Lee, S. Kim, Y. Kim, J. Park, and J. Yi, "Computational design of high efficiency a-Si:H/CIGS monolithic tandem solar cell," *Optik*, vol. 173, pp. 132–138, Nov. 2018, doi: 10.1016/j.ijleo.2018.08.004.

[20] J. He *et al.*, "Structural and optoelectronic properties of a-Si:H: A new analysis based on spectroscopic ellipsometry," *Vacuum*, vol. 146, pp. 409–421, Dec. 2017, doi: 10.1016/j.vacuum.2017.04.013.

[21] J. D. Joannopoulos and M. L. Cohen, "Electronic properties of complex crystalline and amorphous phases of Ge and Si. I. Density of states and band structures," *Phys. Rev. B*, vol. 7, no. 6, pp. 2644–2657, Mar. 1973, doi: 10.1103/PhysRevB.7.2644.

[22] W. B. Jackson, S. M. Kelso, C. C. Tsai, J. W. Allen, and S.-J. Oh, "Energy dependence of the optical matrix element in hydrogenated amorphous and crystalline silicon," *Phys. Rev. B*, vol. 31, no. 8, pp. 5187–5198, Apr. 1985, doi: 10.1103/PhysRevB.31.5187.

[23] S. Prayogi, Y. Cahyono, D. Hamdani, and Darminto, "Effect of active layer thickness on the performance of amorphous hydrogenated silicon solar cells," *Eng. Appl. Sci. Res.*, vol. 49, no. 2, pp. 201–208, 2022, doi: 10.14456/easr.2022.22.

[24] Ö. Pehlivan *et al.*, "Structural and interfacial properties of large area n-a-Si:H/i-a-Si:H/p-c-Si heterojunction solar cells," *Mater. Sci. Semicond. Process*, vol. 22, pp. 69–75, Jun. 2014, doi: 10.1016/j.mssp.2014.02.002.

[25] L. Ley, S. Kowalczyk, R. Pollak, and D. A. Shirley, "X-ray photoemission spectra of crystalline and amorphous Si and Ge valence bands," *Phys. Rev. Lett.*, vol. 29, no. 16, pp. 1088–1092, Oct. 1972, doi: 10.1103/PhysRevLett.29.1088.

[26] S. Prayogi, Y. Cahyono, and Darminto, "Fabrication of solar cells based on a-Si: H layer of intrinsic double (P-i_x-i_y-N) with PECVD and efficiency analysis," *J. Phys. Conf. Ser.*, vol. 1951, no. 1, p. 012015, Jun. 2021, doi: 10.1088/1742-6596/1951/1/012015.

[27] P.Garikepati and T. Xue, "Charge transport in a-Si:H PIN solar cells under AC excitation," *SEM. Sol. Cells*, vol. 27, no. 1, pp. 69–77, Jun. 1992, doi: 10.1016/0927-0248(92)90044-P.

[28] S. Gupta, G. Morell, and B. R. Weiner, "Role of H in hot-wire deposited a-Si:H films revisited: Optical characterization and modeling," *J. Non-Cryst. Solids*, vol. 343, no. 1, pp. 131–142, Sep. 2004, doi: 10.1016/j.jnoncrysol.2004.07.008.